COMMUNICATIONS PHYSICS

ARTICLE

https://doi.org/10.1038/s42005-020-00420-3 OPEN

Time-stretch infrared spectroscopy

Akira Kawai[1], Kazuki Hashimoto[2], Tatsuo Dougakiuchi[3], Venkata Ramaiah Badarla[2], Takayuki Imamura[1], Tadataka Edamura[3] & Takuro Ideguchi[1,2,4]✉

Improving the spectral acquisition rate of broadband mid-infrared spectroscopy promises further advancements of molecular science and technology. Unlike pump-probe spectroscopy, which requires repeated measurements with different pump-probe delays, continuous spectroscopy running at a high spectral acquisition rate enables transient measurements of fast non-repeating phenomena or statistical analysis of a large amount of spectral data. Recently, Fourier-transform infrared spectrometers with rapid delay scan mechanisms including dual-comb spectrometers have significantly improved the measurement rate up to ~1 MSpectra s^{-1} that is fundamentally limited by the signal-to-noise ratio. Here, we overcome the limit and demonstrate the fastest continuous broadband mid-infrared spectrometer running at 80 MSpectra s^{-1} by implementing a wavelength-swept time-stretch spectroscopy technique. Our proof-of-concept experiment demonstrates broadband absorption spectroscopy of phenylacetylene from 4.4 to 4.9 μm (2040–2270 cm^{-1}) at a resolution of 15 nm (7.7 cm^{-1}) with a signal-to-noise ratio of 85 without averaging and a shot-to-shot fluctuation of 1.3%.

[1] Department of Physics, The University of Tokyo, Tokyo, Japan. [2] Institute for Photon Science and Technology, The University of Tokyo, Tokyo, Japan. [3] Central Research Laboratory, Hamamatsu Photonics K.K., Hamamatsu, Japan. [4] PRESTO, Japan Science and Technology Agency, Saitama, Japan. ✉email: ideguchi@ipst.s.u-tokyo.ac.jp

Vibrational molecular spectroscopy has been used as an indispensable tool for investigating molecular systems in a variety of fields. Pump-probe vibrational spectroscopy has brought tremendous advancements in physical and biological chemistry with a femtosecond (fs) to picosecond temporal resolution, but it can be only applicable to repetitively reproducible phenomena with the pump pulses[1–4]. Measuring rapidly changing dynamics, including stochastic or non-repeating phenomena such as gaseous combustion or conformation change of proteins, necessitates high-speed continuous measurement techniques. High-speed continuous measurement is also essential for analyzing a large number of spectra with, for example, raster scan imaging[5] or flow cytometry[6,7]. Among various vibrational spectroscopy techniques, single-detector-based methods have gained an advantage in measurement speed because a fast photodetector with the bandwidth of ~MHz–GHz outperforms the scan rate of a grating-based dispersive spectrometer with a line sensor operated at a rate of ~kHz. In the past couple of decades, we have especially witnessed significant advancements of broadband coherent Raman scattering spectroscopy, but its scan speed is essentially limited by the low signal-to-noise ratio (SNR), resulting in ~1–10 kHz measurement rates[5,8–14].

Mid-infrared (MIR) absorption spectroscopy, the counterpart modality of vibrational spectroscopy to Raman spectroscopy, holds much potential for the high-speed continuous measurement because of its inherently larger cross-section: several orders of magnitude larger than that of the coherent Raman scattering. In the MIR region, where the richest molecular signatures exist, Fourier-transform spectroscopy (FTS) techniques with rapid delay scan mechanisms including dual-comb spectroscopy[15,16] have been the fastest methods to date[17,18]. To the best of our knowledge, the fastest measurements with a sufficient spectral resolution of ~100 GHz for measuring liquid phase molecules and an SNR of ~10–100 were recorded by dual-comb spectroscopy with quantum cascade laser (QCL) combs or microresonator combs, which are operated at acquisition rates of ~MSpectra s^{-1} [19–21]. Importantly, the acquisition rates of these systems are not limited by their instrumental scan rates but SNR[22,23], which fundamentally prevents further improvement. Therefore, to improve the measurement speed, one must use another technique that could provide a better SNR.

Wavelength-swept spectroscopy is known to have an advantage in SNR by a factor proportional to $\sqrt{N}$, where N is the number of spectral elements, against the multiplex measurement such as FTS[24] (details are discussed in Supplementary Note 1). Therefore, especially for broadband spectroscopy with a large N, the SNR advantage becomes significant. In the MIR region, wavelength-swept lasers such as external-cavity QCLs have been demonstrated[25,26], but these lasers have shown limited instrumental scan rates up to 250 kHz[27,28], which provide lower spectral acquisition rates than those of the state-of-the-art dual-comb spectrometers. Now, we recognize that a single-pulse broadband spectroscopy technique called time-stretch (TS) spectroscopy (also known as dispersive Fourier-transform spectroscopy) is an ideal frequency-swept spectroscopy technique that can be operated at a rate of 10 s of MSpectra s^{-1} with a fs mode-locked laser[29]. However, this technique has been demonstrated only in the near-infrared region where advanced telecommunication optics such as extremely low-loss optical fibers and ultrafast photodetectors are available. To the best of our knowledge, it has never been demonstrated in the MIR region due to the lack of suitable technology. To demonstrate MIR TS spectroscopy, there are three components that must be prepared: (1) a high repetition rate MIR fs laser source running at 10 s of MHz, (2) a low-loss TS dispersive optics in the MIR region, and (3) a fast MIR photodetector at a bandwidth of several GHz. Especially, the last two components are technically demanding. For example, an optical fiber, which is usually used as a time stretcher, is too lossy in the MIR region (~100–1000 dB km^{-1}), and bandwidths of commercially available fast MIR photodetectors are too low (~100 MHz–1 GHz). Note that the fast photodetector is not necessarily required for demonstrating the higher SNR of TS spectroscopy, but is needed for achieving the high-speed measurement capability.

In this work, we demonstrate TS infrared (TS-IR) spectroscopy spanning from 4.4 to 4.9 μm running at the fastest acquisition rate of 80 MSpectra s^{-1}, 1–2 orders higher than the previous record enabled by the inherently better SNR of the wavelength-swept spectroscopy. In our system, we use (1) a synchronously pumped fs optical parametric oscillator (fs-OPO) as a MIR light source, (2) a pulse-stretching technique termed free-space angular-chirp-enhanced delay (FACED)[30,31], and (3) a recently developed quantum cascade detector (QCD) with a high −3-dB bandwidth of 5 GHz[32].

Results

TS-IR spectrometer. Our TS-IR spectrometer is schematically shown in Fig. 1. Our light source is a home-made MgO-doped periodically poled lithium niobate (MgO:PPLN) (HC Photonics) fs-OPO pumped with a Ti:Sapphire mode-locked laser running at a repetition rate of 80 MHz (Maitai, Spectra Physics). The OPO cavity is designed for resonating the signal pulses. Wavelength of the MIR idler pulses can be tuned from 2.1 to 5.1 μm by changing the OPO cavity length, the PPLN grating period, and/or the pump wavelength. In this work, we set the center wavelength of the idler pulses at 4.6 μm. An average power of the MIR pulses is 70 mW. The pulse stretching is made by FACED system, which consists of a diffraction grating (219 grooves mm^{-1}, Richardson Gratings), a pair of concave mirrors (f = 100, and 200 mm), and a pair of flat mirrors with a separation distance of d (mm) and an angle of α (degree). All the above optics are coated with gold. In FACED system, wavelength-dependent incident angle of the beam into the flat mirror pair is translated into the chromatic optical path length delay (linear chirp), leading to the pulse stretch from ~100 fs to ~10 ns along with the wavelength-time conversion. The output pulse consists of sub-pulses due to a

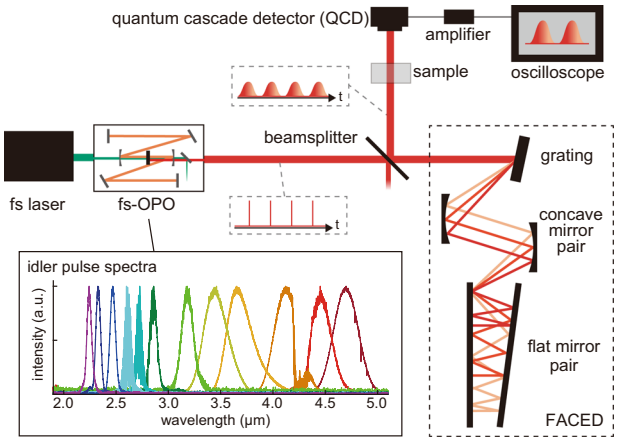

Fig. 1 Schematic of time-stretch infrared (TS-IR) spectrometer. The mid-infrared fs pulse is stretched in the free-space chirp-enhanced-delay (FACED) system and detected by the quantum cascade detector (QCD) after passing through the sample. The QCD signal is amplified and digitized with the fast oscilloscope. The bottom left inset shows the wavelength-tunable spectra of the idler pulses generated by the femtosecond optical parametric oscillator (fs-OPO).

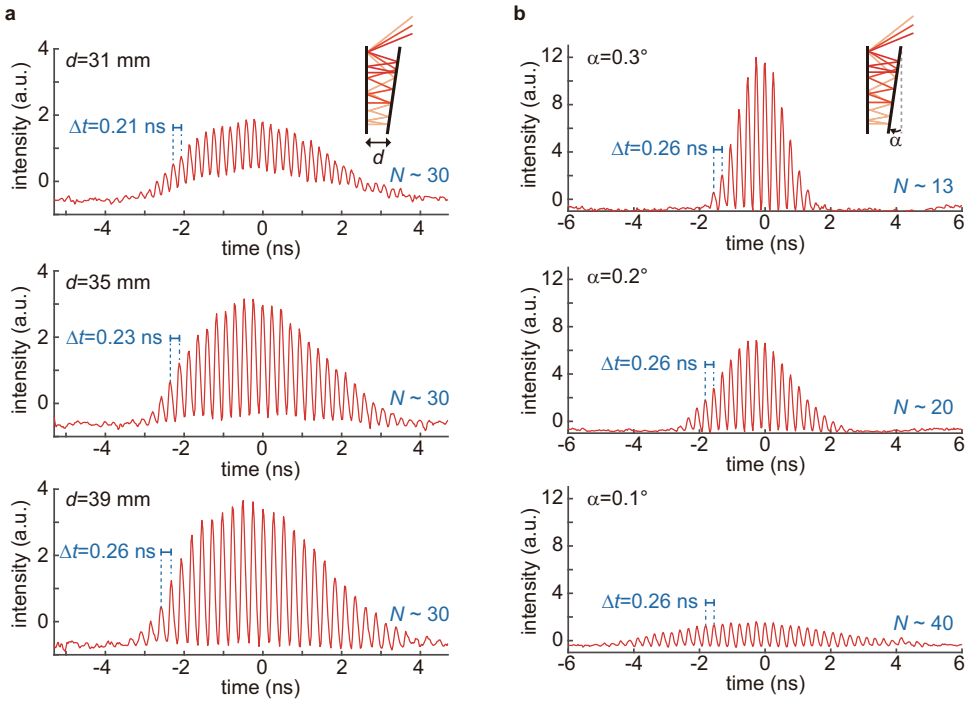

Fig. 2 Characterization of a time-stretched mid-infrared pulse. Stretched pulse waveforms are measured under several conditions of a pair of flat mirrors in the FACED system. **a** Mirror-pair-distance (d) dependence on the temporal interval of the sub-pulses (Δt). The results show good agreement with the theoretical relation, $\Delta t \sim 2d/c$, where c denotes the speed of light. **b** Mirror-pair-angle (α) dependence on the number of sub-pulses (N). The results show good agreement with the theoretical relation, $N \sim \theta/\alpha$, where θ denotes a constant value determined by a FACED geometry.

discrete condition of back reflection at the flat mirror pair. The power throughput of the FACED system is ~9%. This high throughput is especially important in the case of MIR pulse stretching because a conventional technique using a single-mode fiber suffers from significantly large optical loss. The stretched pulses with the average power of 6.3 mW are picked out with a beamsplitter and focused onto a photodetector. We use an uncooled QCD with a −3-dB cutoff frequency of 5 GHz (20 GHz for −20 dB) made by Hamamatsu Photonics K.K. as a fast MIR photodetector. The QCD can be operated with much larger bandwidth than the conventional semiconductor-based detectors due to the short lifetime of the sub-band transitions. Also, the non-biased operation leads to the low noise property. Our detector has sensitivity from 3.3 to 6.0 μm. The QCD signal is amplified by 20 dB with a microwave amplifier with a bandwidth of 0.01–26.5 GHz (Hewlett Packard) and digitized at a sampling rate of 80 GS s^{-1} by a high-speed oscilloscope with a bandwidth of 16 GHz (Teledyne LeCroy).

Characterization of the system. To characterize the system, we first measure the stretched pulse waveform under several conditions of a pair of flat mirrors in our FACED system (Fig. 2). We confirm that change in temporal interval between the adjacent sub-pulses (Δt) depends on the distance between the mirrors (d), which agrees well to the theoretical relation

$$\Delta t \sim 2d/c,$$

where c is the speed of light[30]. We also confirm change in the number of sub-pulses (spectral components) (N) depends on the angle of the mirrors (α)

$$N \sim \theta/\alpha,$$

where θ is a constant value determined by a FACED geometry. In the following experiment, we align the mirror pairs to fulfill the condition, $\Delta t = 0.26$ ns and $N = 30$.

High-speed spectroscopy. To demonstrate spectroscopic capability of TS-IR, we first measure notch-filtered spectra by putting a sharp 0.3-mm beam block near the Fourier plane of the FACED system (Fig. 3a). We confirm that a dip in the waveform shifts by 13 nm in wavelength by shifting the position of the beam block by 0.5 mm in the Fourier plane, which agrees well to the theoretical estimation. Then, we measure absorption spectrum of liquid phenylacetylene. The repetitive broadband time-stretched spectra are clearly observed every 12.5 ns (repetition rate of 80 MHz) as shown in Fig. 3b. The magnified single spectrum (Fig. 3c) shows an absorption line characteristic to the C–C triple bond of the molecules, which agrees well to the reference spectrum measured by a home-made Fourier-transform infrared (FT-IR) spectrometer (Fig. 3d). The spectral resolution is 15 nm (7.7 cm^{-1}), which is determined by spectral gap between the adjacent spectral elements (an experimental verification is shown in Fig. 4), while SNR of the spectrum is evaluated as 85. The shot-to-shot fluctuation of the spectra is evaluated as 1.3% by taking standard deviation of peak intensities of the consecutively measured 40 spectra. The dominant noise source is attributed to the detector and relative intensity noise for lower and higher optical power in our experimental condition, respectively.

To carefully evaluate the spectroscopic capability of TS-IR, we perform additional demonstrations. We first measure multiple absorption lines from different molecular species, a mixture of phenylacetylene and toluene in a 1-mm-thick cuvette with a concentration ratio of 3:47 within the spectral span of the spectrometer (Fig. 4a). A fundamental absorption band of phenylacetylene and an overtone band of toluene are clearly observed, showing the capability of multi-species detection. Next, we evaluate the spectral resolution by measuring a notch-filtered spectrum with narrow linewidth of 13 nm (6.0 cm^{-1}), which is separately evaluated by an FT-IR measurement at a resolution of 10 nm (4.5 cm^{-1}), prepared by sharp beam blocks placed near the Fourier plane. The TS-IR spectrum shows two sharp lines (dips)

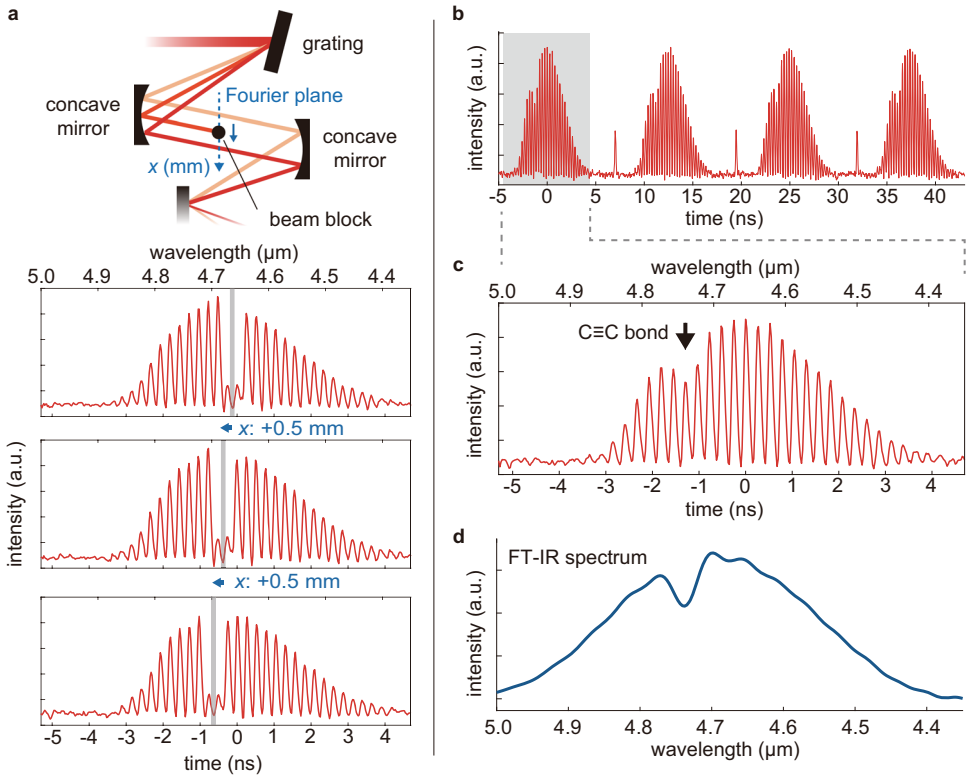

Fig. 3 Time-stretch infrared (TS-IR) spectroscopy. a Top figure shows the optical layout of the notch filter. A sharp 0.3-mm beam block is placed near the Fourier plane of the FACED system. Bottom figures show spectrally filtered TS-IR spectra. The dip in the waveform shifts by 13 nm in wavelength by shifting the position of the beam block by 0.5 mm in the Fourier plane, which agrees well to the theoretical estimation. The gray lines show the positions of the beam block (notch filter). **b** Continuously measured molecular absorption TS-IR spectra of phenylacetylene at a rate of 80 MHz (12.5 ns interval between the adjacent spectra). **c** A magnified spectrum of **b**. An absorption line of the C–C triple bond is clearly observed. **d** A reference absorption spectrum of phenylacetylene measured by Fourier-transform spectroscopy.

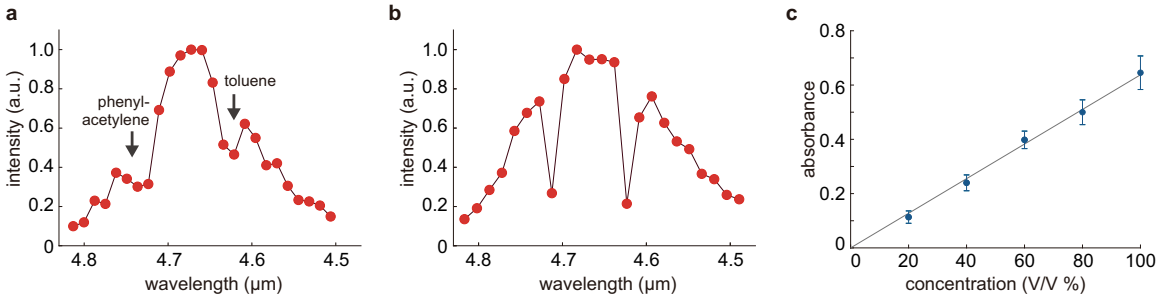

Fig. 4 Performance evaluation of the time-stretch infrared (TS-IR) spectrometer. a A non-averaged TS-IR spectrum of two molecular species, toluene and phenylacetylene. **b** A non-averaged TS-IR spectrum of narrow notch filters. The observed dips with single spectral points indicate that our TS-IR system has a spectral resolution determined by the spectral space between the adjacent spectral point, 15 nm (7.7 cm^{-1}), in this experiment. Errors of the spectral intensities in **a**, **b** are too small to be visible, which are evaluated by the standard deviation of the noise floor. **c** Linear concentration dependence of absorbance evaluated by the average of 30 absorbance spectra of phenylacetylene diluted in toluene. The unit V/V % indicates volume concentration. The error bars are evaluated by the standard deviation of 30 spectra. For the measurements of **a**, **b**, the average power of the optical parametric oscillator output was 55 mW.

with single spectral points, verifying that the resolution is determined by the space between the adjacent spectral points, 15 nm (7.7 cm^{-1}), as theoretically expected (Fig. 4b). Finally, we verify the linear dependence of the absorbance on the molecular concentration by measuring phenylacetylene diluted by toluene in a 100-μm-thick cuvette with different concentrations. Absorbance of a vibrational band of the phenylacetylene is plotted for each concentration in Fig. 4c, showing a linear dependence as expected in linear absorption spectroscopy.

Discussion

The spectroscopic specification of our system can be improved in several directions. First, using a higher repetition rate laser can increase the spectral acquisition rate. Second, the current spectral resolution of 7.7 cm^{-1} is lower than those of previously demonstrated MSpectra s^{-1}-level DCS spectrometers: 0.3 cm^{-1} of QCL-based DCS[20] (note that it is lowered to 2.0–8.0 cm^{-1} to gain the SNR in the actual measurement) and 4.2 cm^{-1} of microresonator-based DCS[21]. However, since it is currently limited by the detector

bandwidth (5 GHz in our case), using a faster detector improves it without sacrificing the measurement speed. Also, simply reducing the repetition rate of the laser leads to resolution improvement without replacing the detector. Third, the spectral bandwidth can be enlarged by using a laser with a broader spectrum and multiple QCDs that cover the broad spectrum. We theoretically discuss the trade-off relation among the SNR, spectral resolution, and spectral sampling rate in Supplementary Note 2.

Potential applications of our ultra-rapid and broadband MIR spectrometer are versatile. For example, in the field of biochemical study on photoreceptive proteins such as rhodopsin where the dynamics of molecular conformation change is studied, the nanosecond to microsecond is a missing time-scale, especially for measuring non-repeatable one-way structural change[2,33]. The TS-IR could open a door to this unexploited field with its continuous high-speed measurement capability. In addition, label-free high-throughput measurements such as liquid biopsy of human blood[34] or flow cytometry for single-cell analysis and sorting[7,35] are also promising directions for future biomedicine because TS-IR's continuous high-speed capability allows us to measure a large number of events within a short time. Furthermore, the TS-IR system can be applied for rapid-scan MIR optical coherence tomography where a larger penetration depth is available than the conventional systems[36].

Methods

Reference spectrum measurement with a home-made FT-IR spectrometer. The reference spectrum shown in Fig. 3d is measured with a home-made FT-IR spectrometer. The FT-IR consists of a home-made Michelson interferometer with a motorized linear delay scanner and a HgCdTe (MCT) detector (PVMI-2TE-10.6-1x1, VIGO System). Optical path length delay of the interferometer is calibrated by a simultaneous measurement of a continuous-wave interferogram with a HeNe laser. The OPO's output is picked out and its spectrum is measured with the phenylacetylene in the cuvette placed after the interferometer. The spectral resolution of the reference spectrum shown in Fig. 3d is 10.5 cm^{-1} without apodization.

Data availability

The data provided in the manuscript are available from T.Id. upon request.

Received: 3 June 2020; Accepted: 7 August 2020;
Published online: 01 September 2020

References

1. Woutersen, A., Emmerichs, U. & Bakker, H. J. Femtosecond mid-IR pump-probe spectroscopy of liquid water: evidence for a two-component structure. *Science* **278**, 658–660 (1997).
2. Herbst, J., Heyne, K. & Diller, R. Femtosecond infrared spectroscopy of bacteriorhodopsin chromophore isomerization. *Science* **297**, 822–825 (2002).
3. Kukura, P., McCamant, D. W. & Mathies, R. A. Femtosecond stimulated Raman spectroscopy. *Annu. Rev. Phys. Chem.* **58**, 461–488 (2007).
4. Bjork, B. J. et al. Direct frequency comb measurement of OD+ CO→ DOCO kinetics. *Science* **354**, 444–448 (2016).
5. Camp, C. H. Jr. & Cicerone, M. T. Chemically sensitive bioimaging with coherent Raman scattering. *Nat. Photon.* **9**, 295–305 (2015).
6. Shapiro, H. M. *Practical Flow Cytometry* (Wiley, New Jersey, 2005).
7. Hiramatsu, K. et al. High-throughput label-free molecular fingerprinting flow cytometry. *Sci. Adv.* **5**, eaau0241 (2019).
8. Arora, R. et al. Detecting anthrax in the mail by coherent Raman microspectroscopy. *Proc. Natl Acad. Sci. USA* **109**, 1151–1153 (2012).
9. Camp, C. H. Jr. et al. High-speed coherent Raman fingerprint imaging of biological tissues. *Nat. Photon.* **8**, 627 (2014).
10. Hashimoto, K. et al. Broadband coherent Raman spectroscopy running at 24,000 spectra per second. *Sci. Rep.* **6**, 21036 (2016).
11. Karpf, S. et al. A time-encoded technique for fibre-based hyperspectral broadband stimulated Raman microscopy. *Nat. Commun.* **6**, 6784 (2015).
12. Saltarelli, F. et al. Broadband stimulated Raman scattering spectroscopy by a photonic time stretcher. *Opt. Express* **24**, 21264–21275 (2016).
13. Ideguchi, T. et al. Microfluidic single-particle chemical analyzer with dual-comb coherent Raman spectroscopy. *Opt. Lett.* **43**, 4057–4060 (2018).
14. Yoneyama, H. et al. CARS molecular fingerprinting using sub-100-ps microchip laser source with fiber amplifier. *APL Photon.* **3**, 092408 (2018).
15. Coddington, I., Newbury, N. & Swann, W. Dual-comb spectroscopy. *Optica* **3**, 414–426 (2016).
16. Ideguchi, T. Dual-comb spectroscopy. *Opt. Photonics N.* **28**, 32–39 (2017).
17. Picqué, N. & Hänsch, T. W. Frequency comb spectroscopy. *Nat. Photon.* **13**, 146–157 (2019).
18. Picqué, N. & Hänsch, T. W. Mid-IR spectroscopic sensing. *Opt. Photonics N.* **30**, 26–33 (2019).
19. Faist, J. et al. Quantum cascade laser frequency combs. *Nanophotonics* **5**, 272–291 (2016).
20. Klocke, J. L. et al. Single-shot sub-microsecond mid-infrared spectroscopy on protein reactions with quantum cascade laser frequency combs. *Anal. Chem.* **90**, 10494–10500 (2018).
21. Yu, M. et al. Silicon-chip-based mid-infrared dual-comb spectroscopy. *Nat. Commun.* **9**, 1869 (2018).
22. Villares, G. et al. Dual-comb spectroscopy based on quantum-cascade-laser frequency combs. *Nat. Commun.* **5**, 5192 (2014).
23. Consolino, L. et al. Fully phase-stabilized quantum cascade laser frequency comb. *Nat. Commun.* **10**, 2938 (2019).
24. Childs, D. T. D. et al. Sensitivity advantage of QCL tunable-laser mid-infrared spectroscopy over FTIR spectroscopy. *Appl. Spectrosc. Rev.* **50**, 822–839 (2015).
25. Tombez, L. et al. Wavelength tuning and thermal dynamics of continuous-wave mid-infrared distributed feedback quantum cascade lasers. *Appl. Phys. Lett.* **103**, 031111 (2013).
26. Borri, S. et al. High-precision molecular spectroscopy in the mid-infrared using quantum cascade lasers. *Appl. Phys. B* **125**, 18 (2019).
27. Lyakh, A. et al. External cavity quantum cascade lasers with ultra rapid acousto-optic tuning. *Appl. Phys. Lett.* **106**, 141101 (2015).
28. Loparo, Z. E. et al. Acousto-optically modulated quantum cascade laser for high-temperature reacting systems thermometry. *Opt. Lett.* **44**, 1435–1438 (2019).
29. Goda, K. & Jalali, B. Dispersive Fourier transformation for fast continuous single-shot measurements. *Nat. Photon.* **7**, 102–112 (2013).
30. Wu, J. L. et al. Ultrafast laser-scanning time-stretch imaging at visible wavelengths. *Light Sci. Appl.* **6**, e16196 (2017).
31. Xu, Y. & Murdoch, S. G. Real-time spectral analysis of ultrafast pulses using a free-space angular chirp-enhanced delay. *Opt. Lett.* **44**, 3697–3700 (2019).
32. Dougakiuchi, T. & Edamura, T. High-speed quantum cascade detector with frequency response of over 20 GHz. *Proc. SPIE* **11197**, 111970R (2019).
33. Lórenz-Fonfría, V. A. et al. Transient protonation changes in channelrhodopsin-2 and their relevance to channel gating. *Proc. Natl Acad. Sci. USA* **110**, E1273–E1281 (2013).
34. Pupeza, I. et al. Field-resolved infrared spectroscopy of biological systems. *Nature* **577**, 52–59 (2020).
35. Zhang, C. et al. Stimulated Raman scattering flow cytometry for label-free single-particle analysis. *Optica* **4**, 103–109 (2017).
36. Israelsen, N. M. et al. Real-time high-resolution mid-infrared optical coherence tomography. *Light Sci. Appl.* **8**, 11 (2019).

Acknowledgements

We thank Makoto Kuwata-Gonokami, Junji Yumoto, and Yu Nagashima for use of their equipment. This work was financially supported by JST PRESTO (JPMJPR17G2), JSPS KAKENHI (17H04852, 17K19071), Research Foundation for Opto-Science and Technology, and Murata Science Foundation.

Author contributions

T.Id. conceived the concept. A.K. designed and constructed the system. A.K., K.H., T.D., and T.Im. performed the experiment. A.K. and K.H. analyzed the experimental data. T.D. and T.E. fabricated and devised the QCD. V.R.B. built the OPO system. T.Id. supervised the entire work. A.K. and T.Id. wrote the manuscript with contributions from all the other authors.

Competing interests

The authors declare no competing interests.

Additional information

Supplementary information is available for this paper at https://doi.org/10.1038/s42005-020-00420-3.

Correspondence and requests for materials should be addressed to T.I.

Reprints and permission information is available at http://www.nature.com/reprints

Publisher's note Springer Nature remains neutral with regard to jurisdictional claims in published maps and institutional affiliations.